Short communication

An inorganic composite membrane as the separator of Li-ion batteries

S.S. Zhang*, K. Xu, T.R. Jow

US Army Research Laboratory, Adelphi, MD 20783-1197, USA

Abstract

We studied an inorganic composite membrane as the separator for Li-ion batteries. Being made of mainly $CaCO_3$ powder and a small amount of polymer binder, the composite membrane has excellent wettability with liquid electrolytes due to its high porosity and good capillarity. Ionic conductivity of the membrane can be easily achieved by absorbing a liquid electrolyte. Additional benefit of such a membrane is that the alkali $CaCO_3$ can scavenge acidic HF, which is inevitably present in the $LiPF_6$-based electrolytes used currently in the Li-ion batteries. In this work, we typically evaluated a membrane with the composition of 92:8 (wt.) $CaCO_3$/Telfon by using a 1.0 m $LiPF_6$ dissolved in a 3:7 (wt.) mixture of ethylene carbonate (EC) and ethylmethyl carbonate (EMC) as the liquid electrolyte. Ionic conductivity of the electrolyte-wetted membrane was measured to be 2.4 mS cm^{-1} at 20 °C versus 8.0 mS cm^{-1} of the liquid electrolyte. With the said membrane as a separator, both Li/graphite and Li/cathode half-cells exhibited good capacity retention. We also found that the Li-ion cell fabricated in this manner not only had stable capacity retention, but also showed good high-rate performance.
© 2004 Elsevier B.V. All rights reserved.

Keywords: Composite membrane; Separator; Ionic conductivity; High-rate performance; Li-ion battery.

1. Introduction

Li-ion batteries have been studied as a potential power source for electric vehicles and hybrid electric vehicles [1,2]. However, high cost and safety concerns still set restrictions to the above application. To reduce cost, most of the previous effort has been focused on developing less expensive materials [3–10], such as spinel $LiMn_2O_4$ cathodes [3], natural graphite anodes [4–9], and liquid electrolytes [10], with little attention paid to the separator. A recent cost estimation of the Li-ion batteries showed that the microporous polyolefin separator, such as polypropylene Celgard® membrane, was 25–30% of the overall cost of Li-ion batteries [11]. Furthermore, the polypropylene membrane will soften or melt as the temperature reaches 130 °C or higher [12]. The resulting volumetric shrinkage of the separator could cause internal short circuits, which may cause catastrophic thermal runaway. Therefore,

the alternative separators that are less expensive and dimensionally stable at elevated temperatures are desired for high-power Li-ion batteries. For the above reasons, we attempted to explore an inorganic composite membrane that is not only less expensive but also thermally more stable. Our original idea was to coat directly the composite membrane on the surface of graphite anode since the Li-ion batteries are intentionally designed as cathode-limited to prevent deposition of the lithium metal with poor cycling efficiency. In the present work, however, we made a self-standing membrane for the purpose of convenient measurements of membrane properties, such as geometric dimensions and ionic conductivity.

On the other hand, it has been well accepted [13,14] that acids are one of the important sources of capacity fading of the cathode materials because acidic HF is inevitably present in the $LiPF_6$-based electrolytes, which so far have been the only choice in the Li-ion batteries. To resolve this problem, we selected alkali $CaCO_3$ as the main component for the composite membrane because it can neutralize acidic products in situ. In this paper, we report the ionic conductivity of

* Corresponding author. Tel.: +1 301 394 0981; fax: +1 301 394 0273.
 E-mail address: szhang@arl.army.mil (S.S. Zhang).

the electrolyte-wetted membrane and explore its application to Li-ion batteries by evaluating cycling performance of the Li half-cells and Li-ion cells.

2. Experimental

The composite membrane was prepared as follows. Using a small amount of ethanol as the diluent, the weighed $CaCO_3$ powder (10 microns, 98%, Aldrich) and Teflon emulsion (61.5% of solid content in water, Du Pont) were thoroughly mixed and hot-rolled into a flexible and self-standing membrane. In this work, a typical membrane with the composition of 92:8 (wt.) $CaCO_3$/Teflon and the thickness of 175–190 μm was made. For electrochemical measurements, the resulted membrane was cut into small disks with an area of 2.85 cm^2. Graphite anode and lithium nickel-based mixed oxide cathode films, provided by Saft America, Inc., were punched into disks with an area of 1.27 and 0.97 cm^2, respectively. All the above disks were dried at 120 °C under vacuum for 16 h before use. The liquid electrolyte used was a solution prepared by dissolving 1.0 m LiPF$_6$ (Stella Chemica Corp) in a 3:7 (wt.) mixture of ethylene carbonate (EC, Grant Chemical) and ethyl methyl carbonate (EMC, Grant chemical). Water content of the electrolyte was determined by Karl–Fisher titration to be 10–15 ppm. In an argon-filled glove box, lithium half-cells and Li-ion cells (2325-type button cells) were assembled and filled with 150 μl of liquid electrolyte by using the composite membrane as a separator. A symmetric cell with stainless steel electrodes was assembled to measure ionic conductivity of the composite membrane.

A Tenney Environmental Oven Series 942 was used to provide a constant temperature environment for the measurement of ionic conductivities at various temperatures. An SI 1287 Electrochemical Interface and an SI 1260 Impedance/Gain-Phase Analyzer were used to measure impedance of the composite membrane, from which the ionic conductivity was calculated. Charge and discharge cycling tests of the cells were performed on a Maccor Series 4000. For rate performance tests, the cells were charged at 0.5 mA and discharged at a specific current. All cycling tests were conducted at room temperature (22–24 °C).

3. Results and discussion

3.1. Ionic conductivity of the composite membrane

The composite membrane is flexible, self-standing, and by itself electrically isolating. We found that the membrane has excellent wettability with all liquid electrolytes tested due to high porosity of the membrane and good capillarity of the $CaCO_3$ particle surface. Therefore, ionic conductivity of the membrane can be easily achieved by absorbing an appropriate amount of liquid electrolyte. Fig. 1
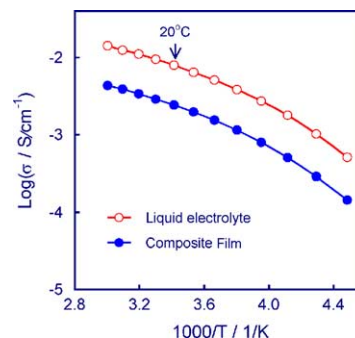

Fig. 1. Arrhenius plots of the ionic conductivities for the electrolyte-wetted membrane and the liquid electrolyte.

shows Arrhenius plots of the ionic conductivities of the electrolyte-wetted membrane and the liquid electrolyte. The electrolyte-wetted membrane has an ionic conductivity of 2.4 mS cm^{-1} at 20 °C versus 8.0 mS cm^{-1} for the liquid electrolyte. We see that conductivities of the membrane and the liquid electrolyte change with the temperature in a very similar manner. This is because the ionic conduction in the membrane is entirely contributed by the liquid electrolyte immobilized in the voids of the membrane. In other words, the ionic conductivity of the electrolyte-wetted membrane is closely associated with the porosity of the composite membrane. In separate work, we have found that ionic conductivity of the electrolyte-wetted membrane can be enhanced significantly by reducing the content of the Teflon binder.

3.2. Cycling performance of the lithium half-cells

Plots of voltage–capacity and differential capacity–voltage for the first two cycles of Li/graphite and Li/cathode half-cells with the composite membrane as the separator are shown in Fig. 2 and Fig. 3, respectively. For the Li/graphite half-cell, coulomb efficiency (CE) of the first two cycles is 90 and 98%, respectively (Fig. 2). The relatively low CE of the first cycle in the Li/graphite cell is due to the formation of a necessary solid electrolyte interface (SEI) on the graphite surface, which is known to involve reductive decomposition of the electrolyte solvents [15]. For the Li/cathode half-cell, the CE of the first two cycles is 86 and 100%, respectively
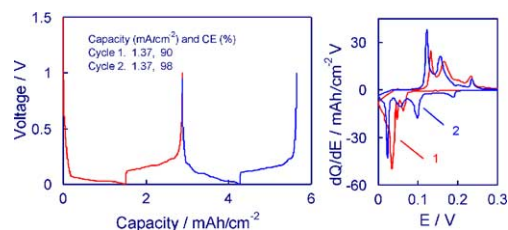

Fig. 2. Plots of voltage–capacity and differential capacity–voltage for the Li/graphite half-cell, which were obtained from the first two cycles at 0.1 mA cm^{-2}.
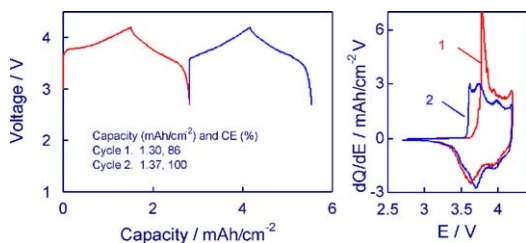
Fig. 3. Plots of voltage–capacity and differential capacity–voltage for the Li/cathode half-cell, which were obtained from the first two cycles at 0.1 mA cm^{-2}.

(Fig. 3). There are two factors relating to the low CE in the first cycle of the Li/cathode cell [16]. One is the irreversibly structural change of the lithium nickel-based mixed oxide cathode material, and the other is the irreversibly oxidative decomposition of the electrolyte solvents. Between these, the latter results in the formation of a resistive SEI. We notice that the CE of the first cycle of the lithium half-cell using the present membrane is very close or even slightly higher than those obtained from the counterpart cells using the conventional Celgard membrane [15,16]. It can be seen in Fig. 2 that the initial lithiation of the Li/graphite cell suffers a bit higher polarization, i.e., the initial peaks of the differential lithiation capacities are shifted to much lower voltage regions. This phenomenon is due to the initially formed SEI at high voltages on the graphite surface is much more resistive than that formed in the low-voltage regions [15]. Because of the rather high polarization during the initial lithiation, we speculate that use of a low current density would be favorable for the forming process of SEI on the graphite surface.

Cycling performances of the Li/graphite and Li/cathode half-cells are shown in Fig. 4. It can be seen that these two cells not only have a matched capacity (1.28–1.30 mAh cm^{-2}), but also show excellent capacity retention with increase in the cycle number. The latter fact reveals that the composite membrane can withstand the potentials at which the graphite and cathode normally operate in the Li-ion batteries. Therefore, we may tentatively conclude that the composite membrane is suitable for the separator of rechargeable Li-ion batteries.
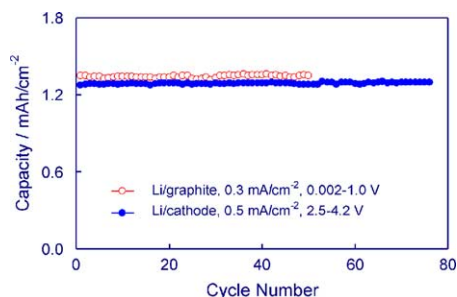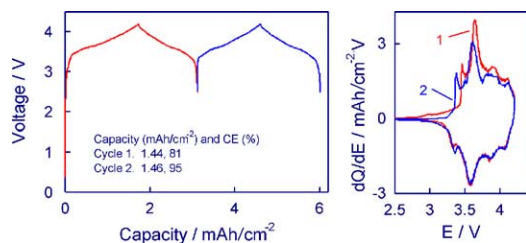

Fig. 5. Plots of voltage–capacity and differential capacity–voltage for the Li-ion cell, which were obtained from the first two cycles at 0.1 mA cm^{-2}.

3.3. Cycling performance of the Li-ion cell

Using the same materials as in half-cells, we assembled a Li-ion cell and then cycled it twice at a low current (0.1 mA cm^{-2}, about C/10 rate) to complete the formation of SEI. Fig. 5 shows plots of voltage–capacity and differential capacity–voltage of these two forming cycles. It is calculated that the CE of the first two forming cycles is 81 and 95%, respectively. As discussed above, in the first cycle both graphite and cathode undergo formation of the SEI, which is known to involve solvent decomposition. That is, the solvents are reduced on the graphite and oxidized on the cathode. From the standpoint of electron flow, they are two opposite electrochemical processes. Therefore, part of the initial irreversibility (19%) of the Li-ion cell, as shown in Fig. 5, can be attributed to the solvent decomposition, which does not consume lithium ions from the limited lithium ion source (cathode). With an increase in the cycle number, the CE of the charge and discharge cycling gradually approached to 100% and remained invariant for the rest of the cycles. Charge and discharge capacities of the Li-ion cell are plotted as a function of the cycle number in Fig. 6, showing that such a cell maintained stable capacity retention.

3.4. High-rate performance of the Li-ion cell

Rate performance of the Li-ion cell was evaluated by charging the cell at a constant current of 0.5 mA and discharging it at various currents. Fig. 7 exhibits the effect of the discharge current on the voltage–capacity profile. It is shown that both capacity and voltage are decreased with increase

Fig. 4. Capacities as a function of the cycle number for the Li/graphite and Li/cathode half-cells. Cycling conditions were shown in the graph.
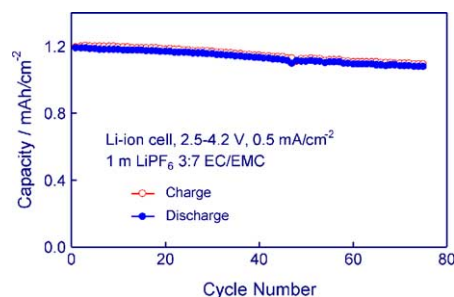

Fig. 6. Charge and discharge capacities of the Li-ion cell as a function of the cycle number, which were measured at 0.5 mA cm^{-2} between 2.5 V and 4.2 V.
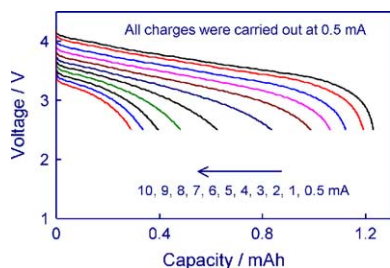
Fig. 7. Voltage–capacity curves of the Li-ion cell at various discharge currents, in which the numbers show the discharge current. Electrode area of the graphite and cathode was 1.27 and 0.97 cm^2, respectively.
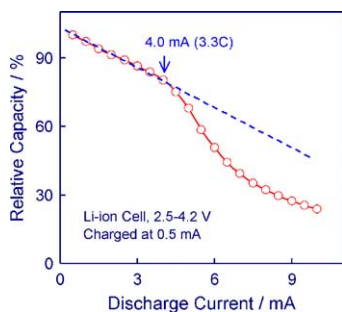

Fig. 8. Correlation of the relative capacity and discharge current for the Li-ion cell.

of the discharge current. This phenomenon can be explained in terms of the electric polarization due to increase in the IR drop. To observe the rate performance, we plot relative capacity of the cell against the discharge current in Fig. 8, in which the relative capacity is defined as a percentage of the discharge capacity at a specific current to the capacity discharged at 0.5 mA. It is observed that the cell retained about 80% of relative capacity even as the discharge current increased to 4.0 mA (3.3 C). Further increase in the discharge current resulted in a significant decrease in the relative capacity. It is known that the reduction of thickness of the composite membrane enhances cycling performance of the cells especially at low temperatures and at high rates. This can be easily achieved by coating directly the composite membrane onto the surface of graphite anode. The results for direct-coated composite membrane will be reported separately.

4. Conclusion

In conclusion, the $CaCO_3$-based composite membrane is a good candidate for an inexpensive and safe separator in rechargeable lithium and Li-ion batteries. Ionic conductivity of the composite membrane can be achieved by absorbing a liquid electrolyte. Ionic conductivity of the electrolyte-wetted membrane is affected mainly by two properties: (1) porosity of the membrane and (2) bulk conductivity of the liquid electrolyte. In batteries, the composite membrane can serve as the microporous separator to physically isolate the anode and cathode without adverse impact on the battery performance. In addition, alkali $CaCO_3$ can neutralize acidic products, which are present in the $LiPF_6$-based electrolytes. For operation of the Li-ion batteries at high current rates, the thickness of the composite membrane should be reduced.

References

[1] M. Brousselya, J.P. Planchata, G. Rigoberta, D. Vireya, G. Sarrea, J. Power Sources 68 (1997) 8.
[2] B. Kennedy, D. Patterson, S. Camilleri, J. Power Sources 90 (2000) 156.
[3] G. Amatuccia, J.M. Tarasconb, J. Electrochem. Soc. 149 (2002) K31.
[4] I.V. Barsukov, F. Henry, P. Zaleski, Joint Meeting of 200th ECS and 52nd ISE, San Francisco, CA, 2–7 September 2001, Abstract No. 306.
[5] K. Zaghib, F. Brochua, A. Guerfia, K. Kinoshitab, J. Power Sources 103 (2001) 140.
[6] H. Wang, M. Yoshio, J. Power Sources 93 (2001) 123.
[7] W. Lu, V.S. Donepudia, J. Prakash, J. Liu, K. Amine, Electrochim. Acta 47 (2002) 1601.
[8] K.K. Guo, Q.M. Pan, S.B. Fang, J. Power Sources 111 (2002) 350.
[9] Y.P. Wu, E. Rahm, R. Holze, J. Power Sources 114 (2003) 228.
[10] T. Takamura, K. Yamaguchi, S. Aoki, A. Shimokawa, K. Sekine, Joint Meeting of 200th ECS and 52nd ISE, San Francisco, CA, 2–7 September 2001, Abstract No. 95.
[11] G. Henriksen, K. Amine, J. Liu, P. Nelson, 204th ECS Meeting, Orlando FL, 12–16 October 2003, Abstract No. 255.
[12] J. Brandrup, E.H. Immergut, Polymer Handbook, third ed., John Wiley & Sons, NY, 1989.
[13] Y. Xia, Y. Zhou, M. Yoshio, J. Electrochem. Soc. 144 (1997) 2593.
[14] D.H. Jang, Y.J. Shin, S.M. Oh, J. Electrochem. Soc. 143 (1996) 2204.
[15] S.S. Zhang, M.S. Ding, K. Xu, J. Allen, T.R. Jow, Electrochem. Solid-State Lett. 4 (2001) 206.
[16] S.S. Zhang, K. Xu, T.R. Jow, Electrochem. Solid-State Lett. 5 (2002) A92.